Astron. Astrophys. 346, 819–830 (1999)

ASTRONOMY AND ASTROPHYSICS

Understanding A-type supergiants

II. Atmospheric parameters and rotational velocities of Galactic A-type supergiants*

E. Verdugo[1], **A. Talavera**[2], **and A.I. Gómez de Castro**[3]

[1] ISO Data Centre, P.O. Box 50727, E-28080 Madrid, Spain (everdugo@iso.vilspa.esa.es)
[2] LAEFF/INTA, P.O. Box 50727, E-28080 Madrid, Spain (ati@laeff.esa.es)
[3] Instituto de Astronomía y Geodesia (CSIC-UCM), Fac. cc. Matemáticas, Universidad Complutense, Av. Complutense s/n, E-28040 Madrid, Spain (aig@orion.mat.ucm.es)

Received 14 October 1997 / Accepted 12 April 1999

Abstract. We present the second paper of a series whose aim is to perform a global study of Galactic A-supergiants. Very little work has been carried out to determine the stellar parameters of these stars. This is illustrated with a brief review of some previous works. In this paper we analyze the determination of absolute magnitudes, spectral types and atmospheric parameters using the most recent Kurucz LTE blanketed model atmospheres and we discuss the applicability of the calibrations, such as the Schmidt-Kaler's (1982) calibration. Rotation is also an important parameter in A-supergiants but their rotational velocities are poorly known. We have calculated projected rotational velocities from the Fourier analysis of the observed Mg II (4481 Å) line.

Key words: stars: atmospheres – stars: fundamental parameters – stars: mass-loss – stars: supergiants

1. Introduction

A-type supergiants are evolved objects, in which substantial mass-loss occurs. However, compared to the amount of work devoted to OB stars, studies of photospheric and wind properties of A-type supergiants are scarce. Because they occupy a region of the HR diagram where evolution is rapid, they are few in number. Furthermore, the effect of the wind in the emergent spectrum of these stars is less pronounced than in O and B supergiants. The mechanisms involved in the mass-loss processes in A-supergiants are still unclear and even the atmospheric parameters (effective temperature and gravity) are only poorly known. These objects are the brightest stars in the visible and can be observed individually in nearby galaxies from large ground based telescopes (Humphreys 1979, 1980; Humphreys & Sandage 1980; Humphreys et al. 1990; Humphreys et al. 1991; Herrero et al. 1994; McCarthy et al. 1995, 1997). This opens up great possibilities for extragalactic studies if we are able to understand them. Such studies have to begin with galactic stars, as these are bright enough to be studied in detail. Moreover they are the evolutionary link between the blue and red supergiants, therefore the study of A-supergiants is very important for the theories of stellar evolution in the upper HR diagram.

This series of papers is based on a large set of observational data obtained by us in the visible and ultraviolet spectral regions. This observational material has allowed us to perform a systematic study of the A-type supergiants atmospheres and winds. Detailed spectra both in the visible and ultraviolet are available in the form of a spectral atlas showing the most representative features of these stars (Verdugo et al. 1999, hereafter Paper I).

Our main purpose is to study the envelope-wind complex of these stars. However, because of A-type supergiants have been scarcely studied in the past our first task is the determination of their basic stellar parameters. In this paper, we present an atmospheric study of 33 A-type supergiants. We discuss previous determinations of their stellar parameters by other authors and the difficulties to model and parameterize effectively their atmospheres. Subsequently, we establish the final parameters which will be used in our future analysis.

In forthcoming papers we shall analyze in detail the complex visible and ultraviolet spectrum of these stars and the applicability of the radiatively driven wind theory to A-supergiants.

1.1. Luminosity of A-type supergiants

A-type supergiants are absent from the solar neighbourhood, and none have reliable parallaxes. The best estimates of absolute magnitude are for stars in clusters or associations, for which distances can be obtained by the method of cluster fitting to determine the main sequence color-magnitude relation (Blaauw 1963). Furthermore, in some associations most of the members

Send offprint requests to: E. Verdugo

* Based on observations made with the INT and JKT telescopes operated on the island of La Palma by the RGO in the Spanish Observatorio del Roque de Los Muchachos of the Instituto de Astrofisica de Canarias, with the 2.2m telescope at Calar Alto Observatory, Spain, with the Bernard Lyot 2m telescope at Pic Du Midi Observatory, France and observations collected at the European Southern Observatory at La Silla, Chile

are evolved stars, and the distance is derived from a mean spectroscopic parallax. Some additional calibration techniques are also available, such as the appearance of O I_{7773} (Parsons 1964; Osmer 1972). In 1925, Merrill noticed the great strength of this triplet in the spectrum of α Cygni (A2 Ia) and since then many authors have stressed the tremendous sensitivity of this feature to the luminosity of the stars. In fact supergiants appear well separated from stars of other luminosity classes in all diagrams based on the intensity of this feature. This blend is appreciably stronger in class Ia supergiants than in class Ib in the spectral type domain B8 to G2; therefore the O I_{7773} is a powerful luminosity criterium. The main factors that affect the intensity of this triplet are: temperature, gravity, microturbulence, NLTE effects and oxygen abundance. The effects of NLTE and microturbulence are discussed in Faraggiana et al (1988). The non-linear dependence of $M_{\rm v}$ and W(O I) and the importance of the temperature in the correlation are analyzed in Arellano Ferro et al. (1991), Arellano Ferro & Mendoza (1993) and Slowik & Peterson (1993).

Other similar calibrations are based on the strength of the Si II lines λ6347 and λ6371 (Rosendhal 1974). There is also a good correlation between the net strength (absorption minus emission) of Hα and luminosity, but the usefulness of this criterion as a luminosity indicator is limited by intrinsic stellar variability and by the fact that the slope of the correlation depends fairly strongly on temperature (Rosendhal 1973). Walker & Millward (1985) have presented a luminosity calibration of W(Hγ) for 31 supergiants. This line is less sensitive to stellar wind and NLTE effects than Hα. Hill et al (1986) recalculated an independent calibration of the $M_{\rm v}$ - W(Hγ) relation by observing 52 OBA supergiants in 25 open clusters with available photometric distance moduli. They found that two superluminous A stars, HD 197345 (α Cygni) and HD 223385 (6 Cas), did not conform to the calibration. The values of $M_{\rm v}$ obtained by these authors by application of the calibration over the selected A-supergiants compared with the photometric values are included in Table 1.

Table 1. $M_{\rm v}$(cal) - W(Hγ) calibration by Hill et al. 1986

Star (HD)	Sp. Type	Cluster (Assoc.)	W (Hγ)	$M_{\rm v}$ (phot)	$M_{\rm v}$ (cal)
12953	A1 Iae	Per OB1	1.55	-7.48	-7.62
13476	A3 Iab	Per OB1	3.35	-6.49	-6.53
14433	A1 Ia	Per OB1	2.47	-7.20	-6.86
14489	A2 Ia	Per OB1	2.64	-7.14	-6.88
20041	A0 Ia	Cam OB1	2.63	-6.22	-6.58
21389	A0 Iae	Cam OB1	1.78	-6.95	-7.33
87737	A0 Ib	Sco-Cen	4.38	-2.78	-5.04
187982	A1 Ia	Vul OB4	2.90	-6.58	-6.51
197345	A2 Iae	Cyg OB7	2.47	-8.99	-7.00
207260	A2 Iae	Cep OB2	2.71	-6.73	-6.83
212593	B9 Iab	Lac OB1	3.23	-4.78	-5.86
223385	A3 Iae^{+}	Cas OB5	1.79	-8.32	-7.63

1.2. Atmospheric parameters and spectral types

Effective temperatures can be determined directly for stars for which both absolute fluxes and apparent radii are known. Direct measurements of the radius are not available for A-supergiants, except for α Cygni (Bonneau et al. 1981). As an alternative approach to estimating $T_{\rm eff}$, Johnson (1966) used color indices to interpolate between stars of earlier and later spectral type with measured angular diameters. Flower (1977) rederived temperature scales and bolometric corrections for stars of all luminosity classes by taking into account ultraviolet and infrared observations. Again, temperatures for the A-type supergiants must be established by interpolation. A more recent calibration based on the previous ones is that of Schmidt-Kaler (1982). However, atmospheric parameters determination of A-type supergiants from photometric color calibrations have large uncertainties. In Garmany & Stencel (1992) the bolometric magnitudes and temperatures are calculated from the intrinsic colors, distances, and derived absolute visual magnitudes using the temperature scale derived for Large Magellanic Cloud stars by Fitzpatrick (1987). Bravo Alfaro et al. (1997) determined the effective temperature of 18 early A-type supergiants using observations on the 13-color photometric system with an average accuracy of about 300 K.

Since during the last decade observational techniques and theoretical models have been drastically improved, observed and theoretical energy distributions can be compared in a more extensive and proper wavelength range than previously and consequently better values of atmospheric parameters can be found. The method for finding the optimum values of $T_{\rm eff}$ and $\log g$ is basically searching for a convergence point of several loci (contours and equivalent widths of Balmer lines, ionization equilibrium, Balmer discontinuity, infrared flux) depicted on the $T_{\rm eff}$ vs $\log g$ plane. This type of analysis has been scarcely applied to A-type supergiants due to the difficulties in modeling their atmospheres.

In Table 2 we show almost all the results obtained by different authors for the atmospheric parameters of A-supergiants.

The first analysis of the atmospheric parameters of A-supergiants from spectroscopic indicators used model atmospheres without line blanketing. Aydin (1972) studied the atmosphere of 6 A-supergiants. He determined the atmospheric parameters of each star by comparing the observed contours and equivalent widths of Hβ and Hγ and the Balmer discontinuity with the same quantities computed with the model atmospheres of Mihalas (1965). Wolf (1971) calculated the atmospheric parameters of HD 87737 using Kurucz's model atmospheres which did not yet include detailed line blanketing.

Modern Kurucz models have been used by a few authors to derive atmospheric parameters of A-supergiants (Lobel et al. 1992; Samedov 1993; Takeda 1994; Takeda & Takeda-Hidai 1995). These works are constrained to very few objects. The most complete analysis over a significant sample of A-supergiants was done by Venn (1995a; 1995b; 1997). She deter-

Table 2. Effective temperatures and gravities of A-type supergiants

HD	$T_{\rm eff}$ (K)	log g	Reference	HD	$T_{\rm eff}$ (K)	log g	Reference
HD 3940	11220		Garmany & Stencel (1992)	HD 197345	9170	1.1	Groth (1961)
	9200	1.4	Venn (1995a)		9900	1.2	Aydin (1972)
HD 5776	10715		Garmany & Stencel (1992)		9500		Nandy & Schmidt (1975)
HD 12953	10233		Garmany & Stencel (1992)		8480		Blackwell & Shallis (1977)
HD 13476	10000		Garmany & Stencel (1992)		10080	1.54	Burnashev (1980)
	8400	1.2	Venn (1995a)		7635		Blackwell et al. (1980)
	8474.4		Bravo Alfaro et al. (1997)		8200		Bonneau et al. (1981)
HD 13744	11749		Garmany & Stencel (1992)		9200	1.1	de Jager et al. (1984)
HD 14433	9550		Garmany & Stencel (1992)		8640		Underhill & Doazan (1982)
HD 14489	12022		Garmany & Stencel (1992)		9100	1.2	Samedov (1993)
	9000	1.4	Venn (1995a)		8500		Theodossiou & Danezis (1991)
	10126.0		Bravo Alfaro et al. (1997)		9550		Garmany & Stencel (1992)
HD 14535	12022		Garmany & Stencel (1992)		9200		Nieuwenhuijzen et al. (1994)
HD 15316	8709		Garmany & Stencel (1992)		10000	1.5	Takeda (1994)
	8350	1.2	Venn (1995a)	HD 207260	9120		Garmany & Stencel (1992)
HD 16778	9550		Garmany & Stencel (1992)	HD 207673	9000		Mihalas (1965)
HD 236995	12022		Garmany & Stencel (1992)		8800	1.04	Aydin (1972)
HD 17378	8709		Garmany & Stencel (1992)		9300	1.75	Venn (1995a)
	7893.8		Bravo Alfaro et al. (1997)		8630.8		Bravo Alfaro et al. (1997)
HD 20041	10091.3		Bravo Alfaro et al. (1997)	HD 209900	9332		Garmany & Stencel (1992)
HD 21389	11000		Aydin (1972)	HD 210221	9800	1.25	Aydin (1972)
HD 46300	9700	1.5	Boyarchuk (1959)		8200	1.3	Venn (1995a)
	9500	1.0	Przybylski (1969)		7687.7		Bravo Alfaro et al. (1997)
	8940/8800		Böhm-Vitense (1982)	HD 212593	9932		Underhill & Doazan (1982)
	10500	2.2	Lambert et al. (1989)	HD 213470	8912		Garmany & Stencel (1992)
	10200	1.9	Lobel et al. (1992)	BD +60 2542	10965		Garmany & Stencel (1992)
	9700	2.1	Venn (1995a)	HD 223385	9300	1.00	Aydin (1972)
HD 59612	8100	1.45	Venn (1995a)		11481		Garmany & Stencel (1992)
	7171.3		Bravo Alfaro et al. (1997)		11481		Garmany & Stencel (1992)
HD 87737	9300	0.9	Boyarchuk (1959)	HD 223960	12303		Garmany & Stencel (1992)
	9500	1.1	Przybylski (1969)				
	9460/8920		Böhm-Vitense (1982)				
	9400		Underhill & Doazan (1982)				
	10500	2.2	Lambert et al. (1989)				
	10200	1.9	Lobel et al. (1992)				
	10400	2.05	Wolf (1971)				
	9700	2.0	Venn (1995a)				
HD 100826	10000		Fitzpatrick & Garmany (1990)				
HD 187983	9486.7		Bravo Alfaro et al. (1997)				

mines atmospheric parameters ($T_{\rm eff}$ and gravity) from spectroscopic indicators. Observed Hγ profiles are compared to those generated from Kurucz's line blanketed model atmospheres (Kurucz 1979), and ionization equilibrium of neutral and ionized magnesium is used to choose the final model parameters. The sample of stars is limited to the lower luminosity class Ib supergiants for which LTE is expected to be a reasonable assumption in calculating the model atmospheres. The validity of this assumption is discussed below.

However, in spite of these efforts, to determine the atmospheric parameters of A-type supergiants a deeper knowledge is required of the stellar photospheres and of the influence of the stellar winds over the spectroscopic indicators (this will be discussed in more detailed below). Moreover, the emergent spectrum of A-supergiants is modified by mass loss and consequently the spectral classification could be affected by the mass loss rate. In Paper I, we present a compilation from the literature of the different assignments of spectral types and luminosity classes to A-type supergiants. The large discrepancies found between different authors reflect the fact that the assignment of a spectral type and luminosity class to an A-supergiant is sometimes difficult and not always unique.

1.3. Rotational velocities of A-supergiants

In 1987, Talavera & Gómez de Castro performed a study of all the A-supergiants observed with the IUE satellite. In this work they detected variable discrete absorption components in the Fe II and Mg II profiles of most of the A-supergiants studied. In 1984, Mullan proposed a wind model which could explain the presence of these narrow and variable components consisting in alternative fast and slow streams similar to the ones observed in the Sun. In this model the shifts of the components would vary and these variations would be modulated by the rotation of the star.

In addition, Kaufer et al. (1996) carried out spectroscopic monitoring over several months of 6 BA-supergiants. They found Hα line profiles highly variable on different timescales ranging from days to months. The time-series analysis reveals timescales up to a factor 6 longer than expected for radial fundamental pulsations periods but consistent with the roughly estimated rotational periods.

These two analyses suggest that rotational modulation could be an interesting source of variability in A-supergiants and this fact would be very useful to discern between the different wind models proposed for these stars. However this possibility remains uncertain until accurate rotational velocities are provided. The rotational velocities of A-type supergiants are poorly known and most of the values come only from the catalogue of Uesugi & Fukuda (1982). In this paper, we present an analysis of the rotational velocities of 31 A-type supergiants from the Mg II λ4481.

2. Program stars and observations

The program stars and the observations are from the *Ultraviolet and Visible Spectral Atlas of A-type supergiants* called Paper I. It contains visible observations of 33 stars of spectral types from A0 to A5 which belong to OB associations or clusters selected from the catalogue of Garmany & Stencel (1992). The basic properties of these stars are given in Table 1 of Paper I. We identify each star by its corresponding entry number in the HD catalogue for easy identification of the stars in the atlas (Paper I).

The observed spectral ranges included the Balmer lines (Hα, Hβ, Hγ and Hδ), Ca II H and K, Na I D and Mg II λ4481 lines. The observations have been carried out in four different campaigns using INT and JKT at La Palma, the 2.2 m Calar Alto telescope and TBL at Pic Du Midi (detailed explanation is given in Paper I). The achieved resolving power ranged from 3700 (JKT) to 38000 (TBL).

The Balmer lines observed have been used in this work as spectroscopic indicators in order to determine the atmospheric parameters. However, the usefulness of these lines is limited by the influence of non-LTE effects, possible mass loss and variability. The Hα line profiles of A-type supergiants present very different shapes, going from symmetric absorption to emission. This line is the most sensitive visible indicator of stellar winds in A-supergiants. Moreover, we found that almost all Hα profiles showing emission are also highly variable (see Paper I).

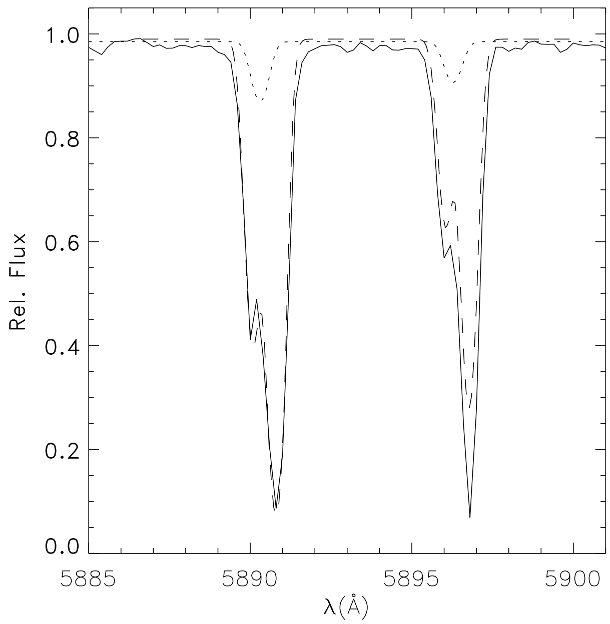

Fig. 1. Na I resonance lines in HD 14535. Stellar contribution is represented with a dotted line and the contribution of two interstellar clouds with a dashed line.

The influence of the stellar wind upon the shape of the lines decreases from Hα down to Hδ. Only five luminous stars of our sample show asymmetric absorption Hβ profiles (HD 12953, HD 14535, HD 21389, HD 223960 and HD 223385) and only one star, HD 223960, displays wind signatures in Hγ and Hδ which also show asymmetric absorption profiles. No evidence of variability has been found in any of these lines.

Photospheric lines can also be reproduced by model atmospheres and therefore used to determine another locus of temperature and gravity. Observed Ca II (3933.663 Å and 3968.468 Å) and Na I (5895.923 Å and 5889.950 Å) resonance lines were used for this purpose. However, we found that these lines are strongly contaminated by the contribution from interstellar clouds. The profile of these lines shows a complex structure with multiple components formed in absorbing regions at different velocities along the line of sight. The resolution of our spectra is not high enough to resolve the velocity structure of the absorbing material and due to the low rotational velocities of the program stars we were unable to separate both contributors to the line profile. A qualitative analysis carried out by us, using model atmospheres (Kurucz 1979) to fit the stellar contribution and the APIG code (Davenhall & Pettini 1990) to model the interstellar clouds, shows that the stellar contribution is dominant in the Ca II profile; however sodium absorption is mainly due to a complex structure in the interstellar medium. An example of such analysis is shown in Fig. 1.

Finally, we have used the Mg II_{4481} line to determine the projected rotational velocities of the stars in our sample (see next section). This line shows symmetric absorption profiles in all the stars studied.

3. Rotational velocities

As mentioned above, rotational modulation caused by corotating surface features (Mullan 1984) may be the source of spectral variability in A-supergiants. However the rotational velocities of these stars are poorly known. We present here a determination of the projected rotational velocities of our sample using Gray's method (Gray 1992).

A standard rotation profile has the following form

$$G(\Delta\lambda) = \frac{2(1-\epsilon)[1-(\frac{\Delta\lambda}{\Delta\lambda_{\rm L}})^2]^{1/2} + \frac{1}{2}\pi\epsilon[1-(\frac{\Delta\lambda}{\Delta\lambda_{\rm L}})^2]}{\pi\Delta\lambda_{\rm L}(1-\epsilon/3)} \quad (1)$$

where $\Delta\lambda = \lambda v \sin i/{\rm c}$ represents the line broadening due to the rotation of the star ($\Delta\lambda_{\rm L}$ is $\Delta\lambda$ at the limbs) and ϵ is the limb-darkening coefficient.

This equation implies the following three assumptions:

- The observational aspect of a uniformly rotating star may be approximated by a circular disk subject to a linear limb-darkening law applicable to all parts of the stellar disk.

- The limb-darkening law for the line is the same as for the continuum.

- The form of the line does not change over the apparent disk.

According to Gray (1992) a normalized line profile can be written

$$\frac{F_{\rm v}}{F_{\rm c}} = H(\lambda) * G(\lambda) \quad (2)$$

where $H(\lambda)$ is the line profile of a nonrotating star convolved with the rotation profile, $G(\lambda)$, to obtain the rotational broadened flux profile.

The Fourier transform of Eq. (2) has the form

$$f_{\rm v} = h(\sigma)g(\sigma) \quad (3)$$

Assuming a value of ϵ=0.6, Carrol (1933a, 1933b) found the transform of $G(\lambda)$ to be

$$g(\sigma) = \frac{J_1(u\beta)}{u\beta} - \frac{3\cos u\beta}{2u^2\beta^2} + \frac{3\sin u\beta}{2u^3\beta^3} \quad (4)$$

in which uβ = $2\pi\Delta\lambda_{\rm L}\sigma$ and J_1 stands for the first-order Bessel function. He noted that g(σ) has zero amplitude at certain Fourier frequencies given by

$$\begin{aligned} \Delta\lambda_{\rm L}\sigma_1 &= 0.660 \\ \Delta\lambda_{\rm L}\sigma_2 &= 1.162 \\ \Delta\lambda_{\rm L}\sigma_3 &= 1.661 \end{aligned} \quad (5)$$

Finding zeros in the Fourier transforms of the line profiles we can determine $\Delta\lambda_{\rm L}$, which is equivalent to $v\sin i$. This method is independent of the instrumental profile since the convolution of the intrinsic spectrum with the instrumental profile may add relative minimum values but will not change the position of the minima given by Eq. (5).

The lines chosen for this analysis should be free of strong pressure broadening, and yet must be strong enough so that the rotation broadened profile can still be seen and measured. For late B through early A type stars, the Mg II 4481 Å line is nearly ideal as long as the rotational broadening is large compared to the 0.2 Å splitting of this triplet (Gray 1992). This type of analysis also requires spectra with high signal-to-noise ratio. We have used here our observed Mg $\rm II_{4481}$ lines to calculate the projected rotational velocities for most of the stars in our sample. An example of this analysis is shown in Fig. 2. In Table 3 we show our results compared with those given by Uesugi & Fukuda (1982) in the catalogue of stellar rotational velocities.

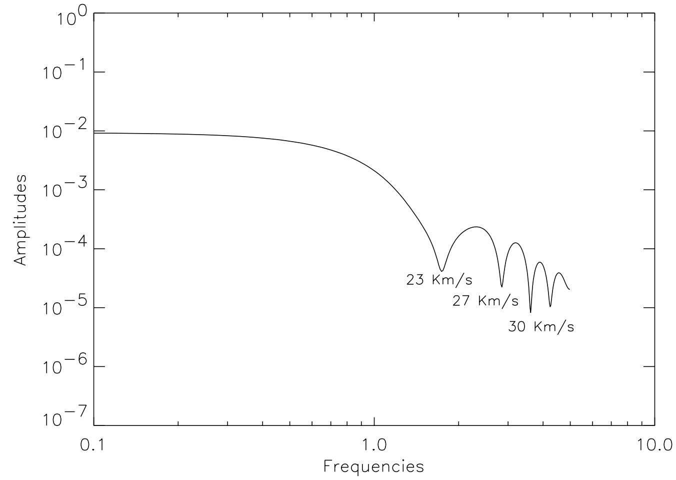

Fig. 2. The rotational velocity analysis of HD 59612.

3.1. Uncertainties of calculated rotational velocities

One of the uncertainties in the calculation of $v\sin i$ comes from the limb-darkening law. We have assumed a linear law with the form

$$I_{\rm c}/I_{\rm c}^0 = 1 - \epsilon + \epsilon\cos\theta \quad (6)$$

where θ is the angle formed by the line of sight and the direction of the emerging flux and $I_{\rm c}^0$ represents the intensity at the stellar disk center. A linear limb-darkening law is a good approximation for our purposes. Non-linear effects are, in most cases, blurred out by other sources of errors.

We have assumed a value of $\epsilon = 0.6$. The influence of the limb-darkening coefficient in the calculated value of $v\sin i$ increases when the rotational velocity increases. For our values this effect is negligible. We have calculated some rotation profiles with different values of ϵ (0.2, 0.4, 0.6 and 0.8) and the Fourier transform of such profiles shows that the position of the frequencies used in the calculation of the rotational velocity do not change although their relative intensity varies. Moreover, according to Wade & Rucinski (1985) the limb darkening coefficient takes a value $0.511 < \epsilon < 0.600$ for temperatures ranging from 8500 K to 10000 K, $\log g$ =1.5 and spectral ranges of $\lambda\lambda$ 4212 - 4687 Å.

The determination of the local continuum is another source of error: a displacement in the continuum level can change the line profile and thus distort the shape of the Fourier transform

Table 3. Rotational velocities ($v \sin i$) in km s^{-1}

Star	This work	Uesugi & Fukuda (1982)
BD +60 51	42	
HD 2928	32	
HD 3940	46	
BD +61 153	37	
HD 4717	22	
HD 5776	29	
HD 12953	49	30
HD 13476	39	50
HD 13744	41	50
HD 14433	47	50
HD 14489	39	10
HD 14535	41	50
HD 15316	30	50
HD 16778	31	
HD 17378	40	35
HD 236995	45	
HD 20041	40	
HD 21389	53	05
HD 46300	23	10
HD 59612	27	20
HD 102878	36	
HD 187982	41	
HD 197345	43	15
HD 207260	44	15
HD 209900	31	
HD 210221	39	30
HD 211971	40	
HD 212593	35	
HD 213470	38	65
BD +60 2542	30	
HD 223960	54	

and modify the position of its zeroes. For our spectra, where the continuum is well defined, this error is almost negligible.

The sampling frequency is another limiting factor in the calculation of $v \sin i$. Defining this frequency as $\sigma_{\rm N} = 0.5/\Delta\lambda$, and considering the spectral resolution, we can get a lowest $v \sin i$ value of $\sim$ 11.5 km s^{-1} and $\sim$ 18 km s^{-1} for Calar Alto and La Palma (INT) spectra respectively. Hence, for stars with $v \sin i$ lower than these values it is not possible to calculate their rotational velocities but only an upper limit.

The intrinsic nature of A-supergiants is the main source of error: the spectral line broadening mechanisms include macroturbulence in these stars. Gray (1975) illustrates the role of macroturbulence in the line profiles of α Cygni (A2 Ia) and concludes that the macrobroadening is large and the analysis in such stars is more complicated. Hence, we conclude that our values in Table 3 can only be considered as upper limits. Some rotational velocities given by Uesugi & Fukuda (1982) (see Table 3) are larger than those given by us. However this is not inconsistent with our upper limits because Gray's method provides direct and independent measurements of $v \sin i$ while the method used by Uesugi & Fukuda (Sletteback et al. 1975) needs to build up a calibration of rotational velocities according to some parameter (e.g. the FWHM).

4. Model atmosphere analysis

As mentioned in the Introduction, very few of the stars in our sample have been studied in detail to derive their atmospheric parameters. A complete atmospheric analysis of A-type supergiants should include effects due to departures from LTE but unfortunately such model atmospheres including detailed line blanketing, which is an important opacity source in A-supergiants atmospheres, are not available. Therefore we have adopted model atmospheres generated by ATLAS9 (Kurucz 1979) which assume plane-parallel geometry, hydrostatic and local thermodynamic equilibrium, and include a very detailed description of line blanketing. Continuous opacity sources relevant at high temperatures (such as electron scattering) and opacities from an extensive list of metal lines are included in the opacity distribution function. Hydrogen line opacities are also included. Apart from non-LTE considerations, additional problems occur with these models due to the fact that A-supergiant atmospheres have very low gravities, near the radiation pressure limit, thus it is difficult to converge the lowest gravity models in hydrostatic equilibrium. Other versions of Kurucz's models (ATLAS6 or ATLAS8) allow lower values of the gravity but the accuracy of the codes is poorer than in ATLAS9. On the other hand, problems related to the circumstellar envelope surrounding these stars are expected to be significant.

Keeping all the above uncertainties in mind, we have tried to assign adequate $T_{\rm eff}$ and $\log g$ values to our program stars.

4.1. Energy distribution and synthetic spectra

Spectroscopic estimates of the atmospheric parameters begin with a comparison of the observed energy distribution with the theoretical emergent fluxes generated from the ATLAS9 code. We have selected two representative stars of our sample: HD 46300 (A0 Ib) and α Cygni (A2 Ia) for such an analysis. For these stars visible fluxes in the range 3200 - 7600 Å were taken from the compilation by Glushneva et al. (1992). For the UV energy distribution, we adopted IUE spectra (1200 - 3200 Å) selected from the database ULDA (Uniform Low Dispersion Archive of IUE spectra).

The interstellar reddening effect from the observed energy distribution was removed using the extintion curves of Code et al. (1976) and the intrinsic color indices given by Fitzgerald (1970). The observed fluxes are then corrected using $E_{\rm B-V} = +0.04$ for α Cygni and +0.02 for HD 46300.

Several models in the range 8500 K $\leq T_{\rm eff} \leq 10000$ K and $1.0 \leq \log g \leq 2.0$ were selected for the comparison. The final models, found to be in reasonable agreement with the observations of α Cyg and HD 46300, were (8500, 1.0) and (10000, 2.0) respectively. The atmospheric parameters found for HD 46300 agree moderately well with the values previously determined from other authors (see Table 2: Lambert et al. (1989); Lobel et al. 1992; Venn 1995a). However, in the case of α Cyg these values are much lower than those determined by other authors (see Table 2; classicaly assigned $T_{\rm eff} \sim 9000$ K and $\log g = 1.5$).

For α Cyg it is not possible to find a unique theoretical spectrum that fits the observed energy distribution. An appreciable ultraviolet flux deficiency at $\lambda \leq 2000$ Å occurs when comparing the observed flux with models of $T_{\rm eff} \geq 9000$ K and a Balmer continuum emission remains in all cases. These discrepancies were already pointed out by Takeda (1994) in a similar analysis of α Cyg using an older version of Kurucz's ATLAS code and they may be related to: i) Uncertainties in $E_{\rm B-V}$. A change of the order of ± 0.05 in $E_{\rm B-V}$ modifies the extintion corrected flux by more than 20% which indicates the importance of accurate values of this parameter; ii) Non-LTE effects. As mentioned above departures from LTE become important for luminous A-type supergiants while for lower luminosity stars, LTE is expected to be a reasonable assumption in calculating the model atmospheres; iii) Circumstellar envelope. The uv flux deficiency can be attributed to the absorption of photospheric photons by the bound-free opacities of neutral species in the circumstellar gas.

The LTE assumption made above for lower luminosity stars, must be considered carefully because, although the model found for HD 46300 assigns atmospheric parameters more reasonable than in the case of α Cyg, the fit of the Balmer jump also shows some discrepancies (see Fig. 3).

Some regions (Ca II and Mg II) of the spectrum of these stars were also fitted using XLINOP, a derivative program of the ATLAS code, with the atomic data given by Kurucz & Peytremann (1975). The synthetic spectra so obtained were convolved with a rotational profile given by Eq. 1.

This analysis provided the same results as the energy distribution fit method; we can fit moderatelly well the spectrum of the lower luminosity star, HD 46300, but the α Cyg lines are not reliably reproduced by the code.

Finally, we have compared the observed Balmer lines with those generated from the program BALMER, another auxiliary program of Kurucz's code.

4.2. Balmer lines

The program BALMER incorporates a detailed Stark broadening theory (Vidal et al. 1973) such that the wings of the Balmer lines can be reliably used to determine atmospheric parameters. In agreement with Venn (1995a) we adopted Hγ as the ideal line for this analysis but, as she argued, in A-type stars the Balmer lines wings depend on both temperature and gravity such that several temperature-gravity pairs may fit an observed profile. As mentioned above, Venn used the ionization equilibrium to choose the final parameters assuming that non-LTE effects can be only moderately significant for lower luminosity A supergiants. However, the discrepancies observed above in the fit of the Balmer jump of HD 46300 (A0 Ib) are probably due to non-LTE effects.

Table 4. Atmospheric parameters ($T_{\rm eff}$ (K), $\log g$)

STAR (HD)	This work	Venn (1995a)	Schmidt-Kaler (1982)
BD +60 51	9000, 1.5	...	9080
BD +61 153	9750, 1.5	...	9730
HD 4717	10000, 2.0	...	9730
HD 5776	9500, 1.0	...	9730
HD 13476	9000, 1.5	8400, 1.20	8770
HD 14489	9000, 1.5	9000, 1.40	9080
HD 46300	9750, 2.0	9700, 2.10	9730
HD 59612	8500, 1.5	8100, 1.45	8510
HD 207673	9000, 1.5	9300, 1.75	9080
HD 209900	9500, 2.0	...	9730
HD 210221	8750, 1.5	8200, 1.30	8770
HD 212593	10000, 1.5	...	10300
BD +60 2542	9000, 1.5	...	9080

We have also fitted the Hα, Hβ and Hδ lines with theoretical profiles to find another locus of temperature-gravity parameters. Hα profiles show wind signatures in the most luminous stars of the sample and they cannot be used in this analysis, even Hγ and Hδ lines of HD 223960 cannot be reproduced by the code, as mentioned above.

The result of this analysis is that only the lines of the less luminous stars (spectral type Ib) can be faithfully reproduced. Examples of the line profile fit are shown in Fig. 4.

For the rest of our program stars we could not find either an adequate model or a unique model to reproduce the line profiles. In some cases the code could not generate models with the low gravities of these stars and in other cases unexpected effects of wind, variability and non-LTE must occur because, although the Hγ profile seems to be symmetric, no combination of temperature-gravity was applicable.

Consequently due to the large amount of stars in our sample for which we are not able to assign a pair ($T_{\rm eff}$, $\log g$), we decided to compare our results with the calibration given by Schmidt-Kaler (1982) as a function of spectral type. Table 4 shows our results obtained with the Balmer lines fits compared with the values found by Venn (1995a) and those given by the calibration. In general the agreement is very good and we can conclude that the calibration of Schmidt-Kaler provides useful values consistent with the uncertainties (typically ± 300 K) which affect the determination of atmospheric parameters in these stars.

It is important to note in Table 4 that our results are closer to the calibration than Venn's values. Probably the parameters calculated by Venn are more accurate and the ionization equilibrium of neutral and ionized magnesium from LTE models can be considered a good approach but unfortunately this approach is only applicable to low luminosity supergiants.

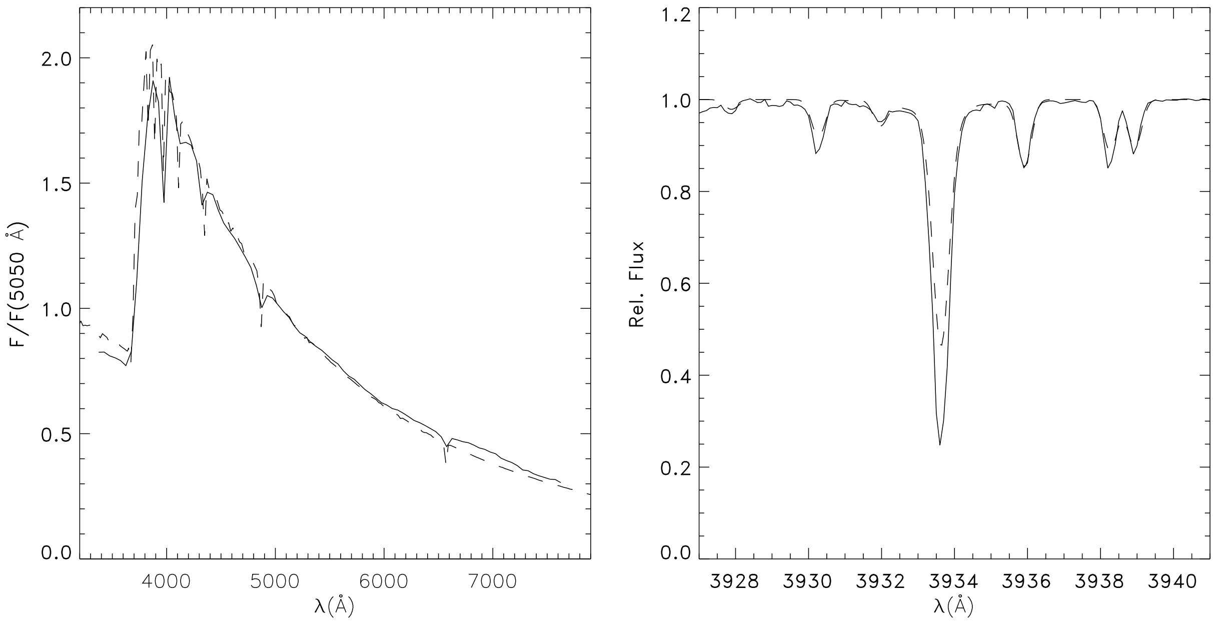

Fig. 3. Sample fits of HD 46300 energy distribution and Ca II K line. Dashed lines correspond to a Kurucz's model of $T_{\rm eff} = 10000$ K and $\log g = 2.0$

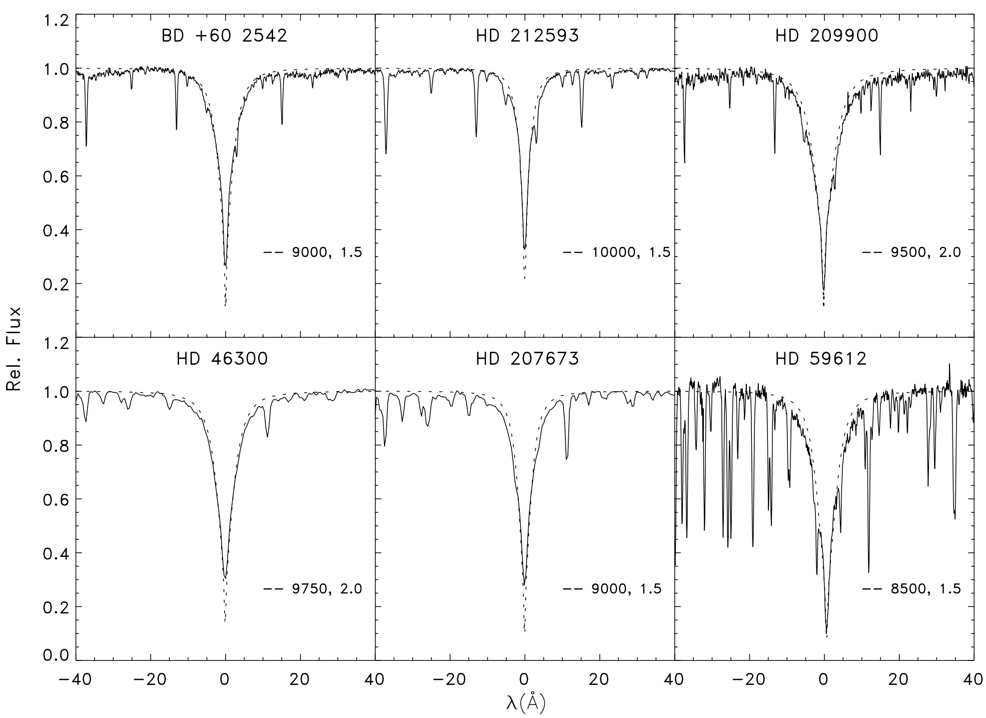

Fig. 4. Some examples of the Hβ (top) and Hγ (bottom) lines fits. Wavelength from 4861 and 4340 respectively.

4.3. Synthetic colors

Kurucz's model atmospheres can also be used to compute synthetic UBV colors and therefore absolute magnitudes and bolometric corrections. We have applied this method for a subset of Kurucz's models in the range $8000\,{\rm K} \leq T_{\rm eff} \leq 10000\,{\rm K}$ and $1.0 \leq \log g \leq 2.0$ which correspond to the stars whose effective temperature and gravity parameters were derived and reported in Table 4.

In computing the theoretical colors we have used the same passband functions and zero points as were used by Buser & Kurucz (1992) for the O to K stars models. The response functions of the bands have been used to calculate the synthetic magnitudes by applying the following expression

$$m_i = -2.5 \log \left(\frac{\int_0^\infty F(\lambda) S_i(\lambda) d\lambda}{\int_0^\infty S_i(\lambda) d\lambda} \right) + C_i \qquad (7)$$

Table 5. Synthetic magnitudes and bolometric corrections

$T_{\rm eff}$	$\log g$	V	Bol	$U-B$	$B-V$	BC
8000	1.0	-20.135	-27.172	-0.013	0.049	-0.051
8000	1.5	-20.142	-27.172	0.058	0.020	-0.044
8000	2.0	-20.142	-27.172	0.105	0.031	-0.044
8500	1.0	-20.285	-27.435	-0.186	0.059	-0.164
8500	1.5	-20.330	-27.435	-0.059	-0.004	-0.119
8500	2.0	-20.339	-27.435	0.004	-0.017	-0.110
9000	1.5	-20.478	-27.683	-0.175	-0.013	-0.219
9000	2.0	-20.498	-27.683	-0.092	-0.040	-0.199
9500	1.5	-20.606	-27.918	-0.280	-0.021	-0.326
9500	2.0	-20.634	-27.918	-0.184	-0.053	-0.298
10000	1.5	-20.723	-28.141	-0.373	-0.029	-0.432
10000	2.0	-20.757	-28.141	-0.266	-0.064	-0.398

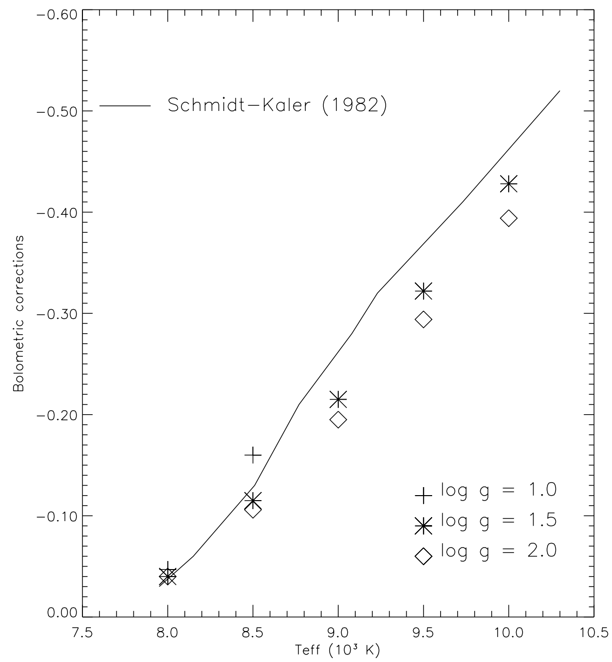

Fig. 5. The theoretical bolometric corrections as compared with the calibration by Schmidt-Kaler (1982).

where $F(\lambda)$ is the flux per unit wavelength, $S_i(\lambda)$ the response function of passband i and C_i is the zero point constant for passband i. The integrals were evaluated numerically by interpolating $S_i(\lambda)$ parabolically and $F(\lambda)$ linearly to a wavelength spacing of 1 Å, then integrating trapezoidally. The results for all the models studied are summarized in Table 5.

According to Buser & Kurucz (1992), the bolometric corrections were calculated using the expression

$$BC = Bol - V + 6.986 \quad (8)$$

where the constant has been adjusted by the smallest value of $Bol - V$ corresponding to the ($T_{\rm eff} = 7000$, $\log g = 1.0$) model, so that the bolometric magnitude is always brighter than the absolute V magnitude.

In order to compare these theoretical bolometric corrections with the values given by the calibration of Schmidt-Kaler, a solar Kurucz model ($T_{\rm eff} = 5770$, $\log g = 4.44$) has been used for defining the zero-point of the bolometric correction. This model provides a BC for the Sun of -0.214, scaled as mentioned above in Eq. (8). The solar bolometric correction given by Schmidt-Kaler (1982) is about -0.21. Hence, the BCs given in Table 5 have to be adjusted by only a small factor of -0.004.

In Fig. 5 we compare the theoretical bolometric corrections calculated with the Kurucz model atmospheres and the calibration of Schmidt-Kaler. This calibration provides bolometric corrections for stars of luminosity class Iab which approximately corresponds to a Kurucz model with gravity of $\sim \log g = 1.5$. We have found good agreement between theoretical and calibrated bolometric corrections in the range $1.5 \leq \log g \leq 2.0$. The major difference occurs in the temperature interval, 9000 K $\leq T_{\rm eff} \leq$ 9500 K and then at a level less than $0^{\rm m}.05$. Kurucz's model atmospheres can not be computed for gravities $\leq \log g = 1.5$ and temperatures higher than 9000 K; therefore this comparison between Kurucz's theoretical predictions and the Schmidt-Kaler calibration can not be extended to the early type A-supergiants with luminosity class Ia. We think, however, that it is reasonable to extrapolate the trend observed in Fig. 5 to these higher temperatures, and henceforth we expect that Kurucz's model atmospheres provide bolometric corrections higher than those given by the Schmidt-Kaler calibration mean relation.

5. Discussion: final adopted parameters

As reported above Kurucz's model atmospheres are only applicable to the less luminous A-type supergiants. For this reason we have to use calibrations in order to assign suitable atmospheric parameters to all the stars in our sample. We have used the values found for the less luminosity stars to study the applicability to A-type supergiants of the calibration given by Schmidt-Kaler (1982). The effective temperatures and the bolometric corrections provided by this calibration are in excellent agreement with the values found from the model atmospheres analysis, indicating that the calibration gives reasonably accurate parameters. Hence, we use the Schmidt-Kaler calibration to assign effective temperatures to all the stars in our sample. Nevertheless, this choice does not overcome the spectral type uncertainties mentioned above for the stars whose atmospheric parameters could not be calculated by using Kurucz's model atmospheres.

The spectral types and luminosity classes have been assigned on the basis of a critical inspection of the values given by different authors (see Table 2 in Paper I). One of the useful characteristics of A-type supergiants is the dependence of the Balmer lines (especially Hα) shape on the luminosity of the star. In Paper I we showed the evolution of the Hα wind pro-

Table 6. Characteristics of the Hα profile, estimated effective temperature from Kurucz's model atmospheres and derived spectral type and luminosity class.

Star	Hα	$T_{\rm eff}$	Sp. T
BD +60 51	AB Symmetric	9000	A2 Ib
HD 2928	AB Asymmetric	$\sim$ 10000	A0 Iab
HD 3940	Emission	$\sim$ 9250	A1 Ia
BD +61 153	AB Symmetric	9750	A0 Ib
HD 4717	AB Symmetric	10000	A0 Ib
HD 5776	AB Symmetric	9500	A0 Ib
HD 12953	P Cygni	$\sim$ 9250	A1 Ia
HD 13476	Emission	9000	A3 Iab
HD 13744	Emission	$\sim$ 10000	A0 Iab
HD 14433	P Cygni		A1 Ia
HD 14489	P Cygni		A2 Iabs
HD 14535	P Cygni		A2 Iabs
HD 15316	Double-peak		A3 Iab
HD 16778	Emission	$\sim$ 9000	A2 Ia
HD 236995	Emission		A0 Ia
HD 17378	Emission	$\sim$ 8750	A5 Ia
HD 20041	Emission		A0 Ia
HD 21389	Double-peak		A0 Ia
HD 46300	AB Symmetric	9750	A0 Ib
HD 59612	AB Asymmetric	8500	A5 Ib
HD 102878	Emission	$\sim$ 9000	A2 Ia
HD 187982	Emission	$\sim$ 9250	A1 Iab
HD 197345	P Cygni	$\sim$ 9000	A2 Ia
HD 207260	Double-peak	$\sim$ 9000	A2 Ia
HD 207673	AB Symmetric	9000	A2 Ib
HD 209900	AB Symmetric	9500	A0 Ib
HD 210221	AB Asymmetric	$\sim$ 8750	A3 Ib
HD 211971	Emission	$\sim$ 9250	A1 Ia
HD 213470	Emission	$\sim$ 8750	A3 Ia
BD +60 2542	AB Symmetric	9000	A2 Ib
HD 223960	Double-peak		A0 Ia+

Note: AB = absorption profiles

file as the luminosity increases in such a way that this property can be used as a powerful discriminator of the luminosity class. Hence, we have chosen the classification which seems to be more consistent with:
(i) The profile of the Balmer lines.
(ii) An approximative value of the effective temperature from Balmer lines fit.

A clear example of the method followed is HD 211971 for which two radically different classifications exist in the literature: A2 Ib (MK system) or A1 Ia (Bouw 1981 from near-infrared spectrophotometry). The Hα profile of this star shows variable emission in the red wing of the line and a shifted component seems to be developing in the blue one. If we accept the MK system assignment to this star, it would be the only Ib star showing such behaviour. In addition, the best fit of the

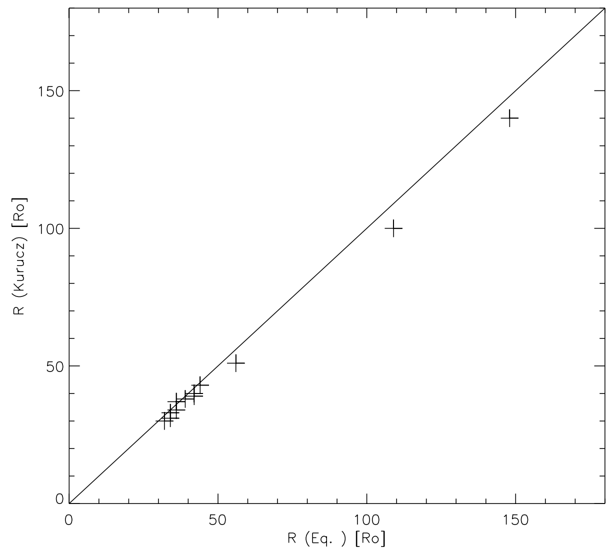

Fig. 6. Radii (in units of solar radius) calculated from Eq. (9) and from model atmospheres analysis

Balmer lines provides an effective temperature of about 9250 K in agreement with a spectral type A1. Therefore we have decided to adopt the A1 Ia classification for this star, in spite of the visual magnitude given by Humphreys (1978) which is smaller than would be expected for an A1 Ia star. This information is summarized in Table 6 for the whole sample.

Finally, in Table 7 we give the final adopted parameters for our sample of stars. The sources for the absolute visual magnitudes are given in the table. Most of them come from the catalogue of Garmany & Stencel (1992) and Humphreys (1978). The masses $M/M_\odot$ were interpolated from evolutionary tracks of Schaller et al. (1992) assuming solar metalicities and assuming that A-type supergiants have evolved directly from the main sequence (Venn 1995b).

Radii can be calculated from

$$M_{\rm bol} = 42.31 - 5\log\left(\frac{R}{R_\odot}\right) - 10\log T_{\rm eff} \quad (9)$$

using the effective temperatures and bolometric corrections given by the calibration of Schmidt-Kaler. We can also compare the values so derived with the determination of radii from model atmospheres analysis matching the absolute visual magnitudes and using the absolute or bolometric flux at the star's surface. Such a comparison has been done for the stars whose atmospheric parameters were calculated and reported in Table 4. As with the agreement found in the previous section for effective temperatures and bolometric corrections, both methods to determine radii provide very similar results. The differences are less than 8% in all the stars analyzed. This is illustrated in Fig. 6.

6. Summary and conclusions

We have analyzed the determination of some stellar parameters in a sample of Galactic A-type supergiants. The main conclusions can be summarized as follows:

Table 7. Stellar parameters

STAR	Sp.T.	$M_{\rm v}$	ref	$M_{\rm bol}$	$T_{\rm eff}$ [K]	$M/M_\odot$	$R/R_\odot$	$v \sin i$ [km/s]
BD+60 51	A2 Ib	-4.8	a	-5.08	9080	9.0	36	42
HD 2928	A0 Iab	-5.5	a	-5.91	9730	8.7	47	32
HD 3940	A1 Ia	-6.37	b	-6.69	9230	14.7	74	46
BD+61 153	A0 Ib	-4.69	b	-5.10	9730	9.0	32	37
HD 4717	A0 Ib	-5.9	c	-6.31	9730	11.9	56	22
HD 5776	A0 Ib	-4.97	b	-5.38	9730	9	36	29
HD 12953	A1 Ia	-7.81	b	-8.13	9230	19.0	144	49
HD 13476	A3 Iab	-7.10	b	-7.31	8770	15.0	109	39
HD 13744	A0 Iab	-6.46	b	-6.87	9730	14.7	72	41
HD 14433	A1 Ia	-6.89	b	-7.21	9230	14.7	94	47
HD 14489	A2 Iabs	-7.84	b	-8.12	9080	23.6	148	39
HD 14535	A2 Iabs	-6.50	b	-6.78	9080	14.7	80	41
HD 15316	A3 Iab	-6.48	b	-6.69	8770	11.8	82	30
HD 16778	A2 Ia	-6.89	b	-7.17	9080	14.7	95	31
HD 236995	A0 Ia	-4.77	b	-5.18	9730	9.0	33	45
HD 17378	A5 Ia	-7.81	b	-7.94	8510	19.2	155	40
HD 20041	A0 Ia	-6.60	a	-7.01	9730	14.7	78	40
HD 21389	A0 Ia	-7.10	a	-7.51	9730	19.3	97	53
HD 46300	A0 Ib	-4.80	a	-5.21	9730	9.0	34	23
HD 59612	A5 Ib	-5.10	d	-5.23	8510	9.0	44	27
HD 102878	A2 Ia	-7.00	e	-7.28	9080	14.7	100	36
HD 187982	A1 Iab	-6.50	a	-6.82	9230	14.7	78	41
HD 197345	A2 Ia	-8.55	b	-8.83	9080	23.6	205	43
HD 207260	A2 Ia	-6.82	b	-7.10	9080	14.7	92	44
HD 207673	A2 Ib	-4.97	f	-5.25	9080	9.0	39	
HD 209900	A0 Ib	-4.85	b	-5.26	9730	9.0	34	31
HD 210221	A3 Ib	-5.00	g	-5.21	8770	9.0	42	39
HD 211971	A1 Ia	-5.50	a	-5.82	9230	8.7	50	40
HD 213470	A3 Ia	-7.30	b	-7.20	8770	14.7	109	38
BD+60 2542	A2 Ib	-5.09	b	-5.37	9080	9.0	42	30
HD 223960	A0 Ia+	-6.90	b	-7.31	9730	19.2	89	54

References:

(a) Humphreys 1978
(b) Garmany & Stencel 1992
(c) Miroshnichenko (priv. comm.)
(d) Talavera & Gómez de Castro 1987
(e) Kaltcheva & Georgiev 1994
(f) Krautter 1980
(g) Blaauw 1963

1. Rotation could be an important stellar wind parameter in A-supergiants, however, the rotational velocities of these stars have been scarcely studied in the past. We have calculated projected rotational velocities ($v \sin i$) from a Fourier analysis of the observed Mg $\rm II_{4481}$ line following the method of Gray (1992). Due to the difficulties in distinguishing between rotational and macroturbulence broadening we conclude that this analysis only provides an upper limit for the true rotational velocities of these stars.

2. Atmospheric parameters of A-type supergiants have been studied from an LTE, line-blanketed model atmospheres analysis. We have compared the observed energy distribution, some photospheric lines and the lines of the Balmer series with the theoretical results computed from Kurucz's model atmospheres. We conclude that this analysis only provides reliable results for the less luminous stars for which the non-LTE and stellar wind effects are less important. This result implys that additional efforts to improve the results on temperatures and gravities of luminous A-type supergiants are useless until models which include effects of wind and departures from LTE with detailed line blanketing are developed.

3. The effective temperatures and bolometric corrections derived for the lower luminosity A-supergiants are in good agreement with the calibration by Schmidt-Kaler (1982). Hence, we have adopted this calibration for the whole sample previous establishment of the spectral types from a critical inspection of the values found in the literature.

We have presented the first results of a large programme intended to study the properties of A-type supergiants. The final parameters established here shall be used to study the stellar wind phenomenology of these stars in a forthcoming paper.

Acknowledgements. We wish to thank Dr. A. Kaufer for having kindly provided unpublished optical data and for his useful comments. We also thank the staff at La Palma, Calar Alto and Pic Du Midi observatories for the kind assistance during the observations. This work was partially supported by DGICYT PB93-491.

References

Arellano Ferro A., Giridhar S., Goswami A., 1991, MNRAS 250, 1
Arellano Ferro A., Mendoza E.E., 1993, AJ 106, 2516
Aydin C., 1972, A&A 19, 369
Blaauw A., 1963, In: Strand K.Aa. (ed.) Basic Astronomical Data. Univ. Chicago Press, Chicago, p. 383
Blackwell D.E., Shallis M.J., 1977, MNRAS 177, 180
Blackwell D.E., Petford A.D., Shallis M.J., 1980, A&A 82, 249
Böhm-Vitense E., 1982, ApJ 191, 255
Bonneau D., Kocchlin L., Oneto J.L., Vakili F., 1981, A&A 103, 28
Bouw G.D., 1981, PASP 93, 45
Boyarchuk A.A., 1959, SvA 3, 748
Bravo Alfaro H., Arellano Ferro A., Schuster W.J., 1997, PASP 109, 958
Burnashev V.I., 1980, Izv. Krym. Astrofiz. Obs. 3, 62
Buser R., Kurucz R.L., 1992, A&A 264, 557
Carrol J.A., 1933a, MNRAS 93, 478
Carrol J.A., 1933b, MNRAS 93, 680
Code A.D., Davis J., Bless R.C., Hanbury Brown R., 1976, ApJ 203, 417
Davenhall A.C., Pettini M., APIG: Absorption Profiles in the Interstellar Gas. A User's Guide, 1990
de Jager C., Mulder P.S., Kondo Y., 1984, A&A 141, 304
Faraggiana R., Gerbaldi M., van't Veer C., Floquet M., 1988, A&A 201, 259
Fitzgerald M.P., 1970, A&A 4, 234
Fitzpatrick E.L., 1987, ApJ 312, 596
Fitzpatrick E.L., Garmany C.D., 1990, ApJ 363, 119
Flower P.J., 1977, A&A 54, 31
Garmany C.D., Stencel R.E., 1992, A&AS 94, 211
Glushneva I.N., Kharitonov A.V., Knyazeva L.N., Shenavrin V.I., 1992, A&AS 92, 1
Gray D.F., 1992, The Observation and Analysis of Stellar Photospheres. Cambridge Univ. Press
Gray D.F., 1975, ApJ 202, 148
Groth H.G., 1961, Z. Astrophys. 51, 321
Herrero A., Lennon D.J., Vílchez J.M., Kudritzki R.P., Humphreys R.H., 1994, A&A 287, 885
Hill G.M., Walker G.A.H., Yang S., 1986, PASP 98, 1186
Humphreys R.M., 1978, ApJS 38, 309
Humphreys R.M., 1979, ApJ 234, 854
Humphreys R.M., 1980, ApJ 241, 587
Humphreys R.M., Sandage A., 1980, ApJS 44, 319
Humphreys R.M., Massey P., Freedman W.L., 1990, AJ 99, 84
Humphreys R.M., Kudritzki R.P., Groth H.G., 1991, A&A 245, 593
Johnson H.L., 1966, ARA&A, 4, 193
Kaltcheva N.T., Georgiev L.N., 1994, MNRAS 269, 289
Kaufer A., Stahl O., Wolf B., et al., 1996, A&A 305, 887
Krautter J., 1980, A&AS 39, 167
Kurucz R.L., 1979, ApJS 40,1
Kurucz R.L., Peytremann E., 1975, Smithsonian Astrophys., Obs. Spec. Rept., No 362.
Lambert D.L., Hinkle K.H., Luck R.E., 1989, ApJ 333, 917
Lobel A., Achmad L., de Jager C., Nieuwenhuijzen H., 1992, A&A 256, 159
McCarthy J.K., Lennon D.J., Venn K.A., et al., 1995, ApJ 455, L135
McCarthy J.K., Kudritzki R.P., Lennon D.J., Venn K.A., Puls J., 1997, ApJ 482, 757
Merrill P., 1925, PASP 37, 272
Mihalas D.M., 1965, ApJS 9, 321
Mullan D.J., 1984, ApJ 283, 303
Nandy K., Schmidt E.C., 1975, ApJ 198, 119
Nieuwenhuijzen H., de Jager C., Cuntz M., 1994, A&A 285, 595
Osmer P.S., 1972, ApJ 171, 393
Parsons S.B., 1964, ApJ 140, 853
Przybylski A., 1969, MNRAS 71, 146
Rosendhal J.D., 1973, ApJ 186, 909
Rosendhal J.D., 1974, ApJ 187, 261
Samedov Z.A., 1993, Astron. Rep. 37, 1
Schaller G., Schaerer D., Meynet G., Maeder A., 1992, A&AS 96, 269
Schmidt-Kaler Th., 1982, Landort-Bornstein, Vol.2, Subvol. b, p. 455, Springer Verlag
Slettebak A., Collins G.W., Boyce P.B., White N.M., Parkinson T.D., 1975, ApJS 29, 137
Slowik D.J., Peterson D.M., 1993, AJ 105, 1967
Takeda Y., 1994, PASJ 46, 181
Takeda Y., Takada-Hidai M., 1995, PASJ 47, 169
Talavera A., Gómez de Castro A.I., 1987, A&A 181, 300
Theodossiou, E., Danezis, E., 1991, Ap&SS, 183, 91
Uesugi A., Fukuda I., 1982, Revised Catalogue of Stellar Rotational Velocities. Department of Astronomy, Kyoto Univ., Kyoto, Japan
Underhill A.B., Doazan V., 1982, B stars with and without emission lines, NASA SP-456
Venn K., 1995a, ApJS 99, 659
Venn K., 1995b, ApJ 449, 839
Venn K., 1997, In: Howarth I. (ed.) ASP Conf. 131
Vidal C.R., Cooper J., Smith E.W., 1973, ApJS 25, 37
Verdugo E., Talavera A., Gómez de Castro A.I., 1999, A&AS 137, 1 (Paper I)
Wade R.A., Rucinski M., 1985, A&AS 60, 471
Walker G.A.H., Millward C.G., 1985, ApJ 289, 669
Wolf B., 1971, A&A 10, 383